Lung Tumor Imaging by Positron Emission Tomography Using C-11 L-Methionine

Kazuo Kubota, Taiju Matsuzawa, Masatoshi Ito, Kengo Ito, Takehiko Fujiwara, Yoshinao Abe, Seiro Yoshioka, Hiroshi Fukuda, Jun Hatazawa, Ren Iwata, Seiichi Watanuki, and Tatsuo Ido

The Research Institute for Tuberculosis and Cancer, and Cyclotron and Radio Isotope Center, Tohoku University, Sendai, Japan

This paper described the first clinical study of lung tumor scanning by positron emission tomography (PET) using C-11-labeled L-methionine (^{11}C-L-Met). Tumor images were clearly visualized by high contrast in eight lung cancer patients and also in a patient with a silicotic nodule. Quantitative evaluations of methionine uptake in tumor tissue and normal tissue by comparing differential uptake ratios suggested that the extent to which ^{11}C-L-Met accumulates in a tumor is closely correlated to the tumor's viability such as benign or malignant, viable or necrotic. ^{11}C-L-Met is considered to be an effective tumor marker for PET diagnosis which represents increased amino acid metabolism of tumors in the mediastinum and lung.

J Nucl Med 26:37–42, 1985

Methionine labeled with Se-75 has been used for many years in nuclear medicine as an agent for pancreas scanning (*1–3*). Its use in tumor imaging has also been studied in parathyroid tumors (*4,5*), lymphomas (*6,7*), thymoma (*8*), hepatomas (*9,10*), neuroblastoma (*11*), and lung cancer (*12,13*). But its diagnostic value is very limited because of high background activity and poor resolution.

Recently, positron emission computed tomography (PET) with C-11-labeled L-methionine (^{11}C-L-Met) has been reported to be valuable when diagnosing pancreas disease (*14,15*). The increase in amino acid incorporation into tumor tissue was experimentally demonstrated using C-14- (*16*) and C-11- (*17*) labeled amino acids, and human brain tumor imagings were also studied by PET using C-11 amino acids (*18,19*). However, it has never been applied to body tumor scanning except a case report which employed it to obtain a clear image of lung cancer (*20*).

This report describes the first clinical study of lung tumor scanning with PET to quantitatively evaluate the uptake of ^{11}C-L-Met in lung cancer and benign tumors.

Received June 14, 1984; revision accepted Oct. 10, 1984.

For reprints contact: Kazuo Kubota, MD, Bldg. 490, Brookhaven National Laboratory, Upton, NY 11973.

MATERIALS AND METHODS

Subjects

As shown in the Table 1, a total of ten subjects were examined. Of these subjects, eight patients had histologically proved advanced lung cancer including seven with squamous cell and one with large cell carcinoma. Of the other two patients, one had a large silicotic nodule and the other had operatively proved tuberculoma. All ten subjects were studied using positron emission tomography ECAT II.* Four patients with lung cancer had been given radiotherapy previously and another four had received no treatment before the PET study. All patients were clinically evaluated in detail including chest x-ray and x-ray computed tomography (CT) to determine the scan level for PET study. The investigation was approved by the clinical research committee of our institution and informed consent was obtained from all subjects.

Radiopharmaceuticals

^{11}C-L-Met used in this study was synthesized from $^{11}CH_3I$ and homocystein following the modified method of Comar et al. (*21*). $^{11}CO_2$ was produced by the proton

TABLE 1
Clinical Study with ^{11}C-L-Met

No.	Disease	Cell type	Radiotherapy (Gy)	RI dose (mCi/kg)	DUR* at 30 min				
					Tumor				
					Benign	Cancer	Muscle	Lung	Blood†
1	Lung cancer	Squamous	0	0.13		2.53	0.51	0.30	0.44
2	Lung cancer	Large	20	0.11		3.55	0.56	0.33	0.39
3	Lung cancer	Squamous	20	0.09		2.63	0.68	0.44	0.50
4	Lung cancer	Squamous	30	0.30		1.67	0.50	0.34	0.43
5	Lung cancer	Squamous	60	0.18		1.93	0.60	0.32	0.63
6	Lung cancer	Squamous	0	0.17		2.41	0.64	0.26	0.47
7	Lung cancer	Squamous	0	0.25		2.17	0.56	0.26	0.54
8	Lung cancer	Squamous	0	0.15		2.10	0.56	0.24	0.52
9	Silicosis			0.24	1.38		0.53	0.45	0.52
10	Tuberculoma			0.27	1.12		0.54	0.41	0.49
Mean				0.19	1.25‡	2.37‡	0.57	0.34	0.49
s.d.				0.07	0.18	0.57	0.057	0.08	0.067

* DUR: Differential uptake ratio

$$\frac{\text{Pixel count/pixel volume}}{\text{Injected RI activity/body weight}} \times \text{calibration factor.}$$

† $\frac{\text{Blood activity/sample weight}}{\text{Injected RI activity/body weight}}$.

‡ $p < 0.05$.

irradiation of a nitrogen gas target system.† $^{11}CH_3I$ was synthesized from $^{11}CO_2$ using an on-line automated system (*22*). Quality assurance tests of ^{11}C-L-Met for clinical use were performed according to the safety guidelines of the clinical research committee of our institution (*23*). The specific activity of ^{11}C-L-Met varied from 5 to 10 mCi/μM at the time of injection and its radiochemical purity was 96% to 99%.

Scanning procedure

Transmission scans were performed using a 2 mCi Ge-68/Ga-68 ring source for the attenuation correction. ^{11}C-L-Met (from 4.8 to 19 mCi, mean 10.9 mCi) in 10 ml of physiological saline was injected intravenously as a bolus. Following the injection, serial emission scans were performed at the slice level through the tumor as determined by CT and transmission scans. The sequences of emission scans varied from 2 to 10 min depending on the injected dose and the time after injection. Scans were finished 45 or 60 min after the injection. Using a medium resolution shadow-shield and filter function, spatial resolution was 14 mm. The scans were corrected for decay and attenuation.

Quantitation of ^{11}C-L-Met concentration was attempted using mean pixel counts in the region of interest (ROI) by the PET scan. Every ROI was carefully determined by using CT and transmission scans as references so that the partial volume effect was minimal and a maximum count recovery was obtained. In each subject, the tumor size was more than 2.5 cm × 3 cm in diameter which corresponded to the count recovery of more than 90% (*24*). To obtain the differential uptake ratios (DUR, previously described as differential absorption ratio) (*25,26*), counts per pixel data were calibrated by the injected dose, body weight, and ECAT-auto well calibration factor.

$$\text{DUR} = \frac{\text{pixel count/pixel volume}}{\text{injected RI activity/body weight}} \times \text{calibration factor}$$

RESULTS

^{11}C-L-Met imaging with PET demonstrated very high radioactivity in all cases of lung cancer. In Case 1, with a 2.5 cm × 3 cm squamous cell carcinoma in the right upper lobe, very high radioactivity appeared in the tumor (Fig. 1a,b). Count ratios per pixel at 30 min were tumor/blood 5.8, tumor/lung 8.4, tumor/muscle 5.0. In Case 2, with a large cell carcinoma, a large homogeneous round mass showed on the CT (Fig. 2b) but a clear ring shaped "hot" region was seen on the PET scan 30 min after injection (Fig. 2a). In Case 4, with squamous cell carcinoma, a ring shaped "hot" region in the lung and increased uptake along the chest wall were shown on the PET scan. Operative findings proved a large central necrotic region corresponding to the center of the ring lesion and chest wall cancer invasion corresponding to the abnormality along the chest on the PET scan. In Case

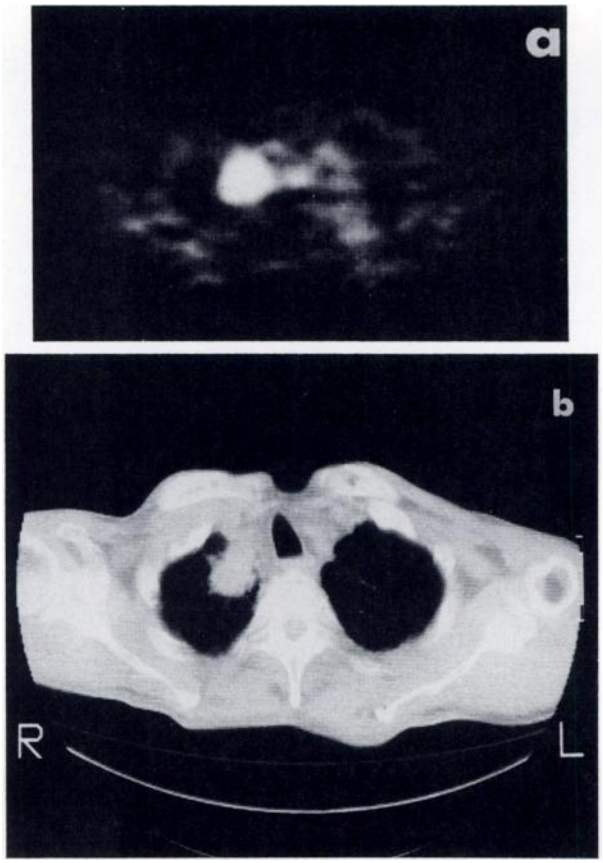

FIGURE 1
a: Case 1. Lung squamous cell carcinoma image obtained with PET 40 min after injection of 7 mCi of ^{11}C-L-Met. b: Chest CT scan showing lung tumor, giving anatomical reference for PET image. (Reprinted by permission of Ref. 20)

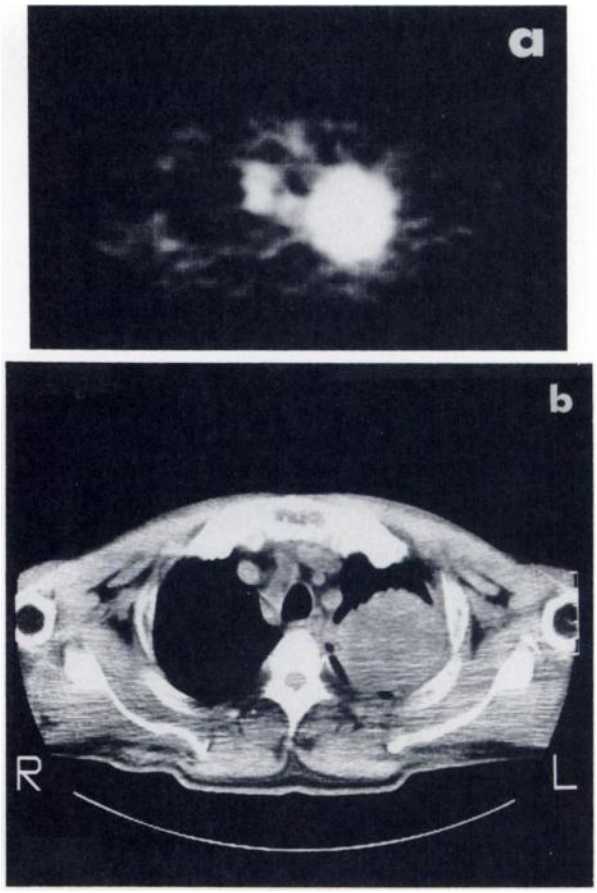

FIGURE 2
a: Case 2. PET image of lung large cell carcinoma 30 min after injection of 6.5 mCi of ^{11}C-L-Met, showing ring-shaped tumor and lymph nodes. b: Chest CT scan showing round homogeneous tumor

9, with a large silicotic nodule in which calcification was diagnosed by chest x-ray and CT, (Fig. 3b), increased accumulation of ^{11}C-L-Met (Fig. 3a) occurred and it was difficult to differentiate this accumulation from the malignant tumor only by observation.

Figure 4 shows the time-activity curves of Case 7, with squamous cell carcinoma. ^{11}C-L-Met in the blood pool decreased rapidly to a plateau at 30 min after injection, whereas its activity in the muscle and in the tumor was almost constant after injection. This demonstrated that the optimum tumor-to-blood ratio can be obtained at 30 min after injection. This case had a lymph node metastasis in the mediastinum which became hotter than the primary tumor. These images are presented in Fig. 5a,b.

Figure 6 shows the time-activity curves for each tumor. In Case 2, with large cell carcinoma, the highest DUR were reached after a rising curve. In Case 10, with a tuberculoma, the lowest and constant values of DUR were seen. The other time-activity curves represented squamous cell carcinoma which showed a wide variation of DURs and time courses.

The DURs of tumor, muscle, lung, and blood in all patients at 30 min after injection are shown in Table 1. Injected doses of ^{11}C-L-Met per body weight had three time variations from 0.09 to 0.30 mCi/kg. But the DURs of the back muscles of each subject remained constant with only a 10% variation (0.57 ± 0.057) and the DURs of the peripheral blood plasma had 13% variation (0.49 ± 0.067) when taken at 30 min after injection. Thus, the DURs were considered to be stable and reliable markers for methionine accumulation in vivo. The average DUR value in lung cancer was 2.37 ± 0.57. The DURs for the tumors of Case 5 which previously received 60 Gy radiotherapy and Case 4 with a large area of necrotic tissue (operatively proved) were lower than those of other lung cancers, but not significantly. The DURs of the benign tumor (1.25 ± 0.18) were significantly lower than the DURs of lung cancer ($p < 0.05$, Mann-Whitney's U-test).

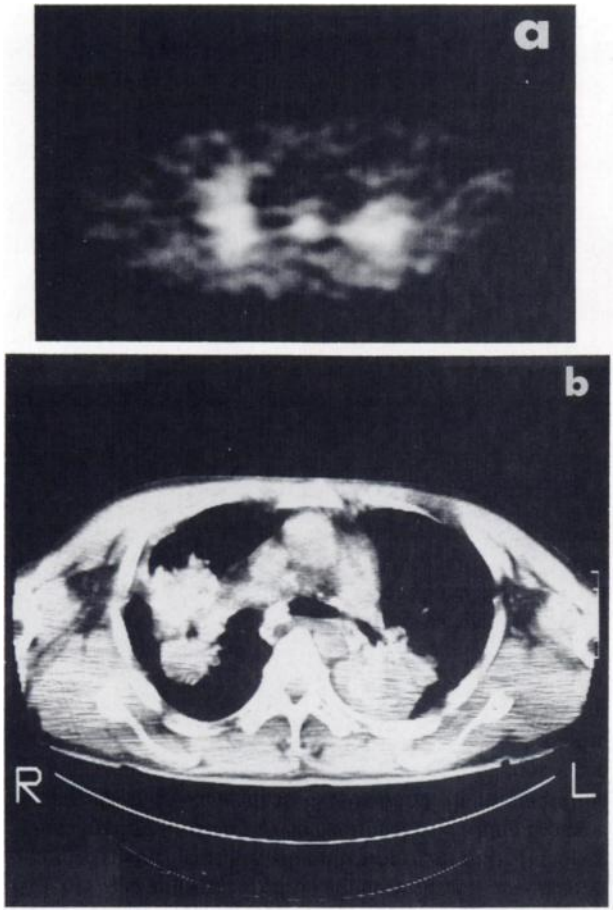

FIGURE 3
a: Case 9. PET image of silicotic nodule 30 min after injection of 12 mCi of ^{11}C-L-Met also showing hot lesion of the nodule. b: Chest CT scan showing nodules in both lungs with calcification

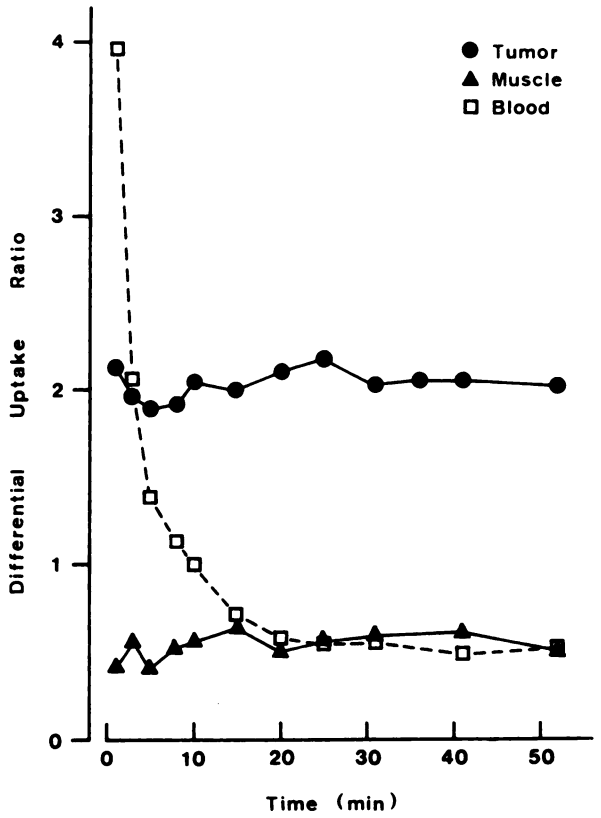

FIGURE 4
Time-activity curves of Case 7, lung squamous cell carcinoma after injection of 13 mCi of ^{11}C-L-Met. Regions of interest were set on PET images, and differential uptake ratios of muscle and tumor were calculated (described in text and Table). Peripheral blood samples were also counted and calculated to get blood clearance curve. (●) Tumor; (▲) Muscle, (□) Blood

DISCUSSION

In this study, all cases of lung cancer were clearly visualized by PET using ^{11}C-L-Met, and the uptake of ^{11}C-L-Met in the tumors and normal tissues were quantitatively evaluated by DURs. In addition, the mean DUR of lung cancer was significantly higher than that of benign tumors suggesting that ^{11}C-L-Met is accumulated in the tumor according to its viability.

Previously, tumor imaging with Se-75 selenomethionine using a conventional scintillation camera was studied in lung cancer (*12,13*) and other tumors (*4–11*). However, its diagnostic value was very limited because Se-75 is a nuclide with long half-life (120 days) so the injected dose must be small (up to 250 μCi) resulting in high background activity which contaminates the tumor image and lowers the resolution. In addition, projected images with conventional scintillation camera are not sensitive to deep lesions in the body. Because of its short half-life (20.4 min), the use of amino acids labeled with C-11 permits the injection of large doses. In this study, a mean injection of ^{11}C-L-Met of 0.19 mCi/kg resulted in a high specific count for tumor imaging with a low background 30 min after injection. Also, by using PET which has improved detection independent of depth, the diagnostic value of ^{11}C-L-Met is greatly increased.

Tumor uptake of ^{11}C-L-Met was expressed by DUR. This was not the rate of protein synthesis but the quantiative assessment of ^{11}C-L-Met uptake in the tissue calibrated by the body weight and injected dose. It was reported that this technique was valid for tumor study (*26*). The DURs of the tumors in this study were closely correlated to whether the tumor was benign or malignant, previously treated or untreated. The DURs of the muscle and blood remained low and very constant with only a 10% and 13% variation, respectively, 30 min after injection. Therefore, we considered DUR to be a useful and reliable marker for comparing methionine uptake in vivo.

The amino acid uptake is high in organs such as the

liver, pancreas, as well as in tumors, but low in the heart, lung, and brain (*17*). Accordingly, tumor imaging with ^{11}C-L-Met forms a high contrast to the surrounding brain (*19*), lung, and mediastinum.

Hayes et al. (*27,28*) reported that the uptake of Ga-67 by soft tissue tumor was mediated by a passive diffusion across the plasma and lysosomal membranes, followed by binding of Ga-67 to lysosomal proteins. Methionine is one of the essential amino acids and uptake by erythrocytes was reported to be mediated by passive transport system across the cell membrane (*29*). Bush et al. (*16*) showed that the largest fraction of injected C-11 amino acids in the tumor was found in the histone fraction. In our preliminary experiment using s.c. rat hepatoma, trichloroacetic acid insoluble fraction of the tumor homogenate reached a very high level shortly after injection of ^{11}C-L-Met. ^{11}C-L-Met uptake seems to be induced by active metabolic utilization of tumor cells such as protein synthesis.

Capillary permeability may increase in tumor tissue, but inactive labeled precursor for D,L-amino acid, ^{11}C-aminonitrile ($H_5C_6NH_2{}^{11}CN$) did not accumulate in the tumor and showed a rapid clearance pattern in most organs (*30*). From this control data, the possibility that ^{11}C-L-Met is only a marker of increased capillary permeability in the tumor seems to be remote.

^{11}C-D,L-valine and ^{11}C-D,L-tryptophan were reported to be effective brain tumor imaging agents using PET (*18*). L-Amino acids labeled with C-11 retain their natural configuration compared to racemic mixtures and to amino acids labeled with Se-75, and are thought to be incorporated into proteins rapidly (*31*). Tumor images obtained by ^{11}C-L-Met also seem to depend on increased protein metabolism.

Brain metabolism of methionine was studied quantitatively using a two-compartment model to determine the rate of protein synthesis (*31*). Further evaluation of tumor imaging dynamics using a rational metabolic model seems to be the next problem to be addressed.

Computed and conventional tomography have made possible the diagnosis of tumors not only in the lung but also in various parts of the body. But these techniques visualize only the shape of abnormality and give no information about the metabolic and biological activity of

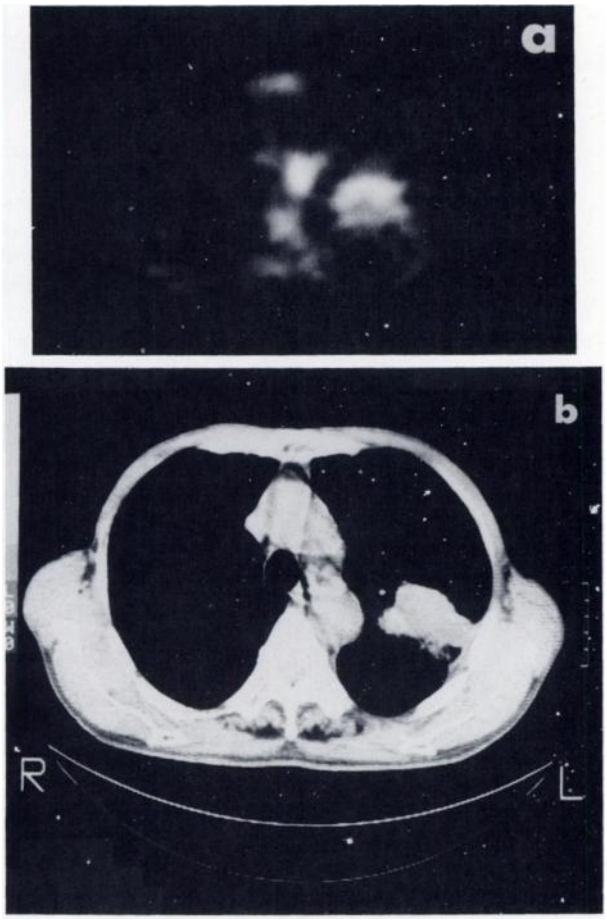

FIGURE 5
Case 7. PET image of lung squamous cell carcinoma 30 min after injection of 13 mCi of ^{11}C-L-Met showing hot lesions in tumor and paraaortic lymph node. b: Chest CT scan of Case 7

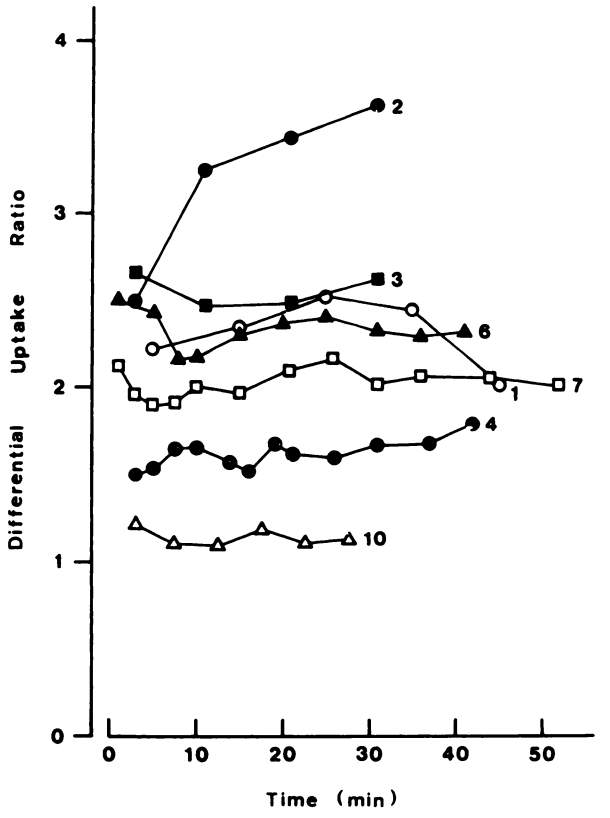

FIGURE 6
Time-activity curves of each tumor. Differential uptake ratio of the tumors were calculated from PET scan data. (○) Case 1; (●) Case 2; (■) Case 3; (◉) Case 4; (▲) Case 6; (□) Case 7; (△) Case 10. Case 5, 8, and 9 were omitted because they were too crowded

the abnormality. In contrast, tumor imaging by PET with ^{11}C-L-Met seems to represent increased protein metabolism of the organ and the tumor's viability. Further metabolic studies with ^{11}C-L-Met will result in useful information for improved cancer diagnosis.

FOOTNOTES

* EG&G, Ortec, USA.

† 166 cm AVF cyclotron, Tohoku University, Sumitomo, Japan.

ACKNOWLEDGMENTS

The authors thank Drs. M. Fujioka, H. Orihara, K. Ishii, and K. Sera for the use of Tohoku University's Cyclotron. They also thank Dr. S. Fujimura, T. Kondo, and their patients for their cooperation and are grateful to Mr. Y. Sugawara for the photography.

This work was supported by a grant-in-aid for scientific research, Ministry of Education, Science and Culture, Japan.

REFERENCES

1. Blau M, Manske RF, Bender MA: Clinical experience with ^{75}Se-selenomethionine for pancreas visualization. *J Nucl Med* 3:202, 1962
2. Blau M, Bender MA: ^{75}Se-selenomethionine for visualization of the pancreas by isotope scanning. *Radiology* 78:974, 1962
3. Haynie TP, Svoboda AC, Zuidema GD: Diagnosis of pancreatic disease by photoscanning. *J Nucl Med* 5: 90-94, 1964
4. DiGiulio W, Beierwaltes WH: Parathyroid scanning with selenium 75 labeled methionine. *J Nucl Med* 5: 417-427, 1964
5. Potchen EJ: The preoperative identification of the abnormal parathyroid—Current status. *Radiology* 88: 1170-1174, 1967
6. Herrera NE, Gonzalez R, Schwartz RD, et al: ^{75}Se methionine as a diagnostic agent in malignant lymphoma. *J Nucl Med* 6:792-804, 1965
7. Spencer RP, Montana G, Scanlon GT, et al: Uptake of selenomethionine by mouse and in human lymphomas, with observations on selenite and selenate. *J Nucl Med* 8:197-208, 1967
8. Toole JF, Witcofski R: Selenomethionine ^{75}Se scan for thymona. *JAMA* 198:1219-1220, 1966
9. Eddleston ALWF, Rake MO, Pagaltsos AP, et al: ^{75}Se-selenomethionine in the scintiscan diagnosis of primary hepatocellular carcinoma. *Gut* 12:245-249, 1971
10. Stolzenberg J: Uptake of ^{75}Se-selenomethionine by hepatoma. *J Nucl Med* 13:565-566, 1972
11. D'Angio GJ, Loken M, Nesbit M: Radionuclear (^{75}Se) identification of tumor in children with neuroblastoma. *Radiology* 93:615-617, 1969
12. Goel Y, Sims J, Pittman JA: Mediastinum scanning with ^{75}Se-selenomethionine. *J Nucl Med* 12:644-645, 1971
13. Critchly M, Testa HJ, Stretton TB: Combined use of ^{99m}technetium-labelled macroaggregates of albumin and ^{75}selenium-selenomethionine in the diagnosis of lung cancer. *Thorax* 29:421-424, 1974
14. Syrota A, Comar D, Cerf M, et al: [^{11}C] methionine pancreatic scanning with positron emission computed tomography. *J Nucl Med* 20:778-781, 1979
15. Syrota A, Duquesnoy N, Pavaf A, et al: The role of positron emission tomography in the detection of pancreatic disease. *Radiology* 143:249-253, 1982
16. Busch H, Davis JR, Honig GR, et al: The uptake of a variety of amino acids into nuclear proteins of tumors and other tissues. *Cancer Res* 19:1030-1039, 1959
17. Kubota K, Yamada K, Fukuda H, et al: Tumor detection with carbon-11-labelled amino acids. *Eur J Nucl Med* 9:136-140, 1984
18. Hübner KF, Durvis JT, Mahaley SM, et al: Brain tumor imaging by positron emission computed tomography using ^{11}C-labeled amino acids. *J Comput Assist Tomogr* 6:544-550, 1982
19. Bergström M, Collins VP, Ehrin E, et al: Discrepancies in brain tumor extent as shown by computed tomography and positron emission tomography using [^{68}Ga]-EDTA, [^{11}C]glucose and [^{11}C]methionine. *J Comput Assist Tomogr* 6:1062-1066, 1983
20. Kubota K, Ito M, Fukuda H, et al: Cancer diagnosis with positron computed tomography and carbon-11-labelled L-methionine. *Lancet* ii:1192, 1983
21. Comar D, Cartron JC, Maziere M, et al: Labelling and metabolism of methionine-methyl-^{11}C. *Eur J Nucl Med* 1:11-14, 1976
22. Iwata R, Ido T: Automated synthesis of $^{11}CH_3I$. CYRIC Annual Report, Tohoku University, 1981, 135-139
23. Clinical Research Committee, Tohoku University: The guideline for quality control of cycrotron produced radiopharmaceuticals. Tohoku University, February, 1982
24. Ito M, Sato T, Hatazawa J, et al: Further evaluation of ECAT II. CYRIC Annual Report, Tohoku University, 1982, pp 213-219
25. Marrian DH, Maxwell DR: Tracer studies of potential radiosensitizing agents. Tetrasodium 2-[C-14]-methyl-1:4-naphthohydroquinone diphosphate. *Br J Cancer* 10:575-582, 1956
26. Fukuda H, Matsuzawa T, Ito M, et al: Clinical evaluation of cancer diagnosis with ^{18}F-2-fluoro-D-glucose. Its usefulness in liver and pancreas cancers. CYRIC Annual Report, Tohoku University, 1983, pp 244-250
27. Hayes RL, Rafter JJ, Byrd BL, et al: Studies of the in vivo entry of Ga-67 into normal and malignant tissue. *J Nucl Med* 22:325-332, 1981
28. Hayes RL, Rafter JJ, Carlton JE, et al: Studies of the in vivo uptake of Ga-67 by an experimental abscess: Concise communication. *J Nucl Med* 23:8-14, 1982
29. Hagenfeldt L, Arvidsson A: The distribution of amino acids between plasma and erythrocytes. *Clin Chim Acta* 100:133-141, 1980
30. Iida S, Iwata R, Ido T: A novel synthesis of no carrier added ^{11}C-DL-amino acid. CYRIC Anual Report, Tohoku University, 1981, pp 115-117
31. Bustany P, Sargent T, Saudubray JM, et al: Regional human brain uptake and protein incorporation of ^{11}C-L-methionine studied in vivo with PET. *J Cereb Blood Flow Metab* (Suppl) 1:S17-S18, 1981